Electrodynamics of $Nd_{1.85}Ce_{0.15}CuO_4$: Comparison with Nb and $YBa_2Cu_3O_{7-\delta}$

Steven M. Anlage, Dong-Ho Wu, J. Mao, S. N. Mao, X. X. Xi, T. Venkatesan, J. L. Peng, and R. L. Greene

Maryland Center for Superconductivity Research, Physics Department, University of Maryland, College Park, Maryland 20742-4111

We have measured the surface impedance of $Nd_{1.85}Ce_{0.15}CuO_4$ (NCCO) thin films and single crystals, $YBa_2Cu_3O_{7-\delta}$ (YBCO) single crystals, and Nb single crystals. We find that the electrodynamic properties of Nb are in good agreement with s-wave BCS theory. YBCO single crystals show behavior which has been seen only in very high quality materials and which is clearly not consistent with s-wave BCS theory. Both thin films and single crystals of NCCO have been grown, thoroughly characterized, and measured at microwave frequencies. We find an unusual degree of consistency in the results between thin films and crystals of NCCO. We also find a surprisingly good agreement between the temperature dependence of the surface impedance, and single-gap BCS s-wave calculations over the entire temperature range. These results are puzzling in the light of the fact that NCCO is a cuprate superconductor, and the crystals were grown in a manner very similar to those of YBCO. We discuss these results and consider a variety of ideas currently in the literature which may explain these striking differences.

INTRODUCTION

Recently, a variety of experimental and theoretical results suggesting a d-wave pairing-state symmetry for the ground state of the high-temperature superconductors have revitalized the ongoing debate on the pairing mechanism of the high-T_c cuprates. In contrast to earlier experimental observations and interpretation in terms of an s-wave BCS behavior in the hole-doped cuprate superconductors (although there was no clear low-temperature exponential activation of the surface resistance and penetration depth), recent results suggest a singlet d-wave pairing state below T_c. For example, magnetic penetration depth measurements of $YBa_2Cu_3O_{7-\delta}$ (YBCO) crystals shows $\lambda(T) \propto T$ at low temperature,[1] suggesting a large density of low-energy quasiparticle states, which is consistent with nodes in the energy gap. The highly anisotropic energy gap seen in the ab plane of $Bi_2Sr_2CaCu_2O_8$ (Bi2212) in an angle-resolved photoemission experiment[2] and linear T dependence of the surface resistance of YBCO crystals at low temperatures[3,4] also support a non-s-wave symmetry gap. Universal observation of high values of the residual microwave surface resistance, $R_s(0)$,[5,6] also points to the existence of many low-energy quasiparticle states, which may be consistent with a non-s-wave pairing state. Moreover, measurements of a quadratic increase of $\lambda(T) \propto T^2$ at low temperatures in YBCO films[7-9] and Bi2212 crystals[10,11] have been attributed to disorder in a d-wave superconductor with nodes. If one accepts the existence of nodes in the energy gap, then from photoemission experiments it would appear that the most likely pairing-state symmetry is $d_{x^2-y^2}$.

These observations and interpretations pose central questions not only for the fundamental physics of cuprates, but also for their applications. Applications of superconductors at high frequencies rely mainly on their low surface resistance properties along with the frequency-independent magnetic penetration depth. Understanding the physics of these materials is essential for engineering systems such as superconducting particle accelerators, and superconducting microwave devices. If the cuprates are s-wave superconductors, then their surface resistance, at least in principle, can be made arbitrarily small by perfecting the material and going to low enough temperatures. Whereas if the cuprates are d-wave superconductors, there is a finite minimum resistance for pure materials,[12-14] and disorder and defects play a central role in determining the magnitude of the surface impedance.[14-16] In either case, since both the order parameter and the microstructure strongly influence the physical properties of the cuprates, studies identifying the order-parameter symmetry along with a detailed understanding of the microstructure and property relations are increasingly important.

To address these issues, much experimental and theoretical work has been performed on the hole-doped superconductors, in particular $YBa_2Cu_3O_7$. Despite the scrutiny, experiments have not yet built up a consistent phenomenological picture identifying the nature of the superconducting state in the cuprates. In addition to interpretations with a d-wave picture, measurements of the penetration depth of YBCO have been interpreted in terms of a finite energy gap over the entire Fermi surface,[17] as evidence for "gapless" behavior,[18] or as a manifestation of weak links between grains.[8,19] Measurements of the surface resistance of YBCO are highly sample dependent, although some results on films are consistent with a small but finite energy gap.[17] The confusion regarding the electrodynamic properties of YBCO is due, in part, to its unique microstructure-property relations. Its short coherence length can easily give rise to a plethora of weak-link phenomena,[19] while the presence of twin boundaries can interrupt the highly conductive Cu-O chains in the structure.

In the electron-doped $Nd_{1.85}Ce_{0.15}CuO_4$ (NCCO), the coherence length is considerably longer than in the other cuprates, and there is a single Cu-O plane layer per unit

cell with no Cu-O chains and no twinning. Hence, if one can deal with the materials idiosyncrasies in the NCCO system, (such as the problems of inhomogeneous Ce and oxygen distribution throughout the sample), the material is more ideal for studying the intrinsic electrodynamics of the cuprates. Because of its many advantages, we have performed a careful and systematic study on the electrodynamics of the NCCO system.[20] However, the recent development of experimental and theoretical work in favor of a d-wave picture calls for a more detailed and careful reexamination of our previous experimental work on the electrodynamics of NCCO system, as well as a quantitative comparison with other superconducting materials. In this paper we report experimental results on the temperature dependence of the penetration depth $\lambda(T)$ and the surface resistance $R_s(T)$ of high-quality NCCO samples, measured at 9.6 GHz. We also report a direct comparison of the data with the results obtained from Nb and YBCO samples.

Our earlier NCCO samples all had rather large residual losses at low temperatures.[20] This invited the question of whether or not we were measuring the intrinsic properties of these materials, or some extrinsic artifact. Other investigators contend that our results reflect those of a very disordered d-wave superconductor.[12] Since our earlier work, we have continued to improve the quality of our NCCO thin films. Consequently we have achieved a very low residual surface resistance, while at the same time obtaining essentially identical results for the temperature dependence of $R_s(T)$ and $\lambda(T)$, and very similar values for the electrodynamic parameters. The detailed temperature dependence and the values of parameters are compared with those obtained from a typical s-wave BCS superconductor, Nb, and also a typical hole-doped cuprate, YBCO.

SAMPLE PREPARATION

Our studies of the electrodynamics of NCCO were performed with both single crystals and thin films. NCCO single crystals were grown by the directional solidification technique.[21] The initially fabricated single crystals (thickness $\sim 30-50$ μm) show a sharp transition (≤ 0.2 K wide) at $T_c \sim 20-22$ K in low-field dc superconducting quantum interference device (SQUID) measurements. While they show no evidence of the $Nd_{0.5}Ce_{0.5}O_{1.75}$ (NCO) impurity phase or superlattice regions,[22] the initially fabricated nominal crystals show multiple superconducting transitions when studied at low-field microwave frequencies as shown in Fig. 1(a). A procedure was developed to remove the surface layers of the crystals by means of an HCl and ethanol etching, and reanneal, until we obtained a single transition in the microwave measurements. In Fig. 1(b), we compare the superconducting transition of the etched NCCO single crystal with that of an as-fabricated NCCO thin film. Note that both the crystal and the film show a single sharp transition. It is important to note that the as-fabricated NCCO thin films did not show multiple superconducting transitions. We believe that this etch and anneal process is needed for crystals because it serves to create more homogeneous Ce and O distribution on the surface of the crystals. This is in accord with microstructure studies on thick as-grown NCCO crystals.[23] It was found that several such treatments were required to obtain single-phase response and low residual losses at microwave frequencies. After the polishing and annealing treatments, single crystals were reduced to typical dimensions of about 2×2 mm^2 and 10–20 μm thick. Independent dc resistivity measurements show that normal resistivity $\rho_n(T_c)$ of the crystals was ~ 100 $\mu\Omega$ cm (Ref. 24) just above T_c and the temperature dependence of $\rho_n(T) \propto T^2$ was followed up to 200 K, typical of previous results.[25]

We have previously studied thin films of NCCO on $LaAlO_3$ substrates.[20] Although $LaAlO_3$ has acceptable microwave loss properties, it is not as good as sapphire in our microwave measurements. Also it is found that there is a considerable lattice mismatch between NCCO and $LaAlO_3$, and that a-axis-oriented grains and an impurity
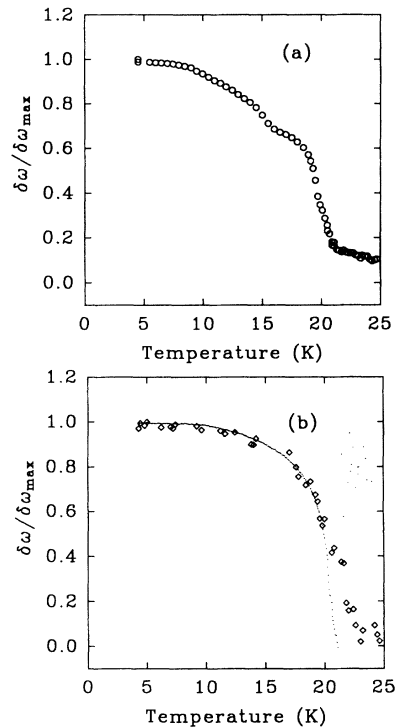
FIG. 1. Low-field ($H_{rf} < 1$ Oe) microwave frequency shift measurements for single crystals and a thin film of NCCO. (a) multiple superconducting transitions of a typical as-grown NCCO crystal. (b) single superconducting transition of the NCCO single-crystal (diamonds) after etching and annealing. Also shown in the frequency shift for an as-grown NCCO thin film (dots). Note that the thin film and the etched single crystal display essentially identical frequency shift behavior in the temperature range below T_c. The dip in the frequency shift of the thin film is associated with trivial finite thickness effects in the film. The crystal and the thin film show similar behavior in Q measurements as well. Low-field dc magnetization measurements showed no evidence of multiple superconducting transitions in all cases.

ELECTRODYNAMICS OF $Nd_{1.85}Ce_{0.15}CuO_4$: COMPARISON ...

phase are present in these films.[31]

To improve this situation, we fabricated new and higher quality NCCO films on sapphire substrates with an yttria-stabilized zirconia (YSZ) buffer layer. Details of the fabrication and sample characterization of the c-axis-oriented thin films on $LaAlO_3$ and sapphire substrates are discussed elsewhere.[26-29] In brief, the NCCO films were prepared on the substrates by pulsed laser deposition in an N_2O atmosphere. For the new films, a YSZ buffer layer approximately 1000 Å thick was deposited on sapphire prior to NCCO deposition. Careful microstructure analysis with x-ray diffraction, and both plane-view and cross-sectional transmission electron microscopy, reveal that the NCCO grains crystallize in the T' structure with the c axis normal to the substrate.[30,31] The only impurity phase detected was $Nd_{0.5}Ce_{0.5}O_{1.75}$ (NCO), a cubic insulating material. NCO is present in grain sizes of a few hundred angstroms at about 1% volume level (or less) in the new films. The impurity amount is about the same as we found in the highest quality thin films on $LaAlO_3$.[30] Also, contrary to films on $LaAlO_3$,[31] no 110-oriented T' grains were found in the thin films on sapphire by TEM investigation.[30,31] In addition, the superlattice modulation seen in polycrystalline bulk samples is completely absent in our thin film samples.[30] Finally, there is evidence from cross-sectional TEM of a 30-Å-thick NCCO/YSZ alloy phase at the interface between these two materials.[31] This alloy serves to reduce the lattice mismatch in the YSZ [001]-NCCO [001] growth direction, and is not thought to significantly affect the microwave results presented in this paper. The films show a sharp transition (< 0.2 K wide) with $T_c \sim 21.5$ K by low-frequency ac susceptibility. The typical dimensions of thin film samples on $LaAlO_3$ were 2.5×5.5 mm^2 with a film thickness of about 5000 Å, while new films on buffered sapphire have the dimensions $\sim 3 \times 5$ mm^2 with a thickness of 2500-2700 Å.

X-ray ϕ scans on the NCCO films show no evidence[29] of the 45° misoriented grains which are so abundant and correlated with high residual losses in YBCO films on MgO substrates.[5] Also, x-ray rocking curve measurements show in-plane misorientation between grains to be less than 0.4°, quite good compared to YBCO films. Rutherford backscattering (RBS) channeling yields on the films are as low as 9%, indicative of good quality, but not quite as good as the best YBCO films, which show a 3% channeling yield.[29] The higher channeling yield is indicative of a greater density of point defects in NCCO films as compared to YBCO films.

Besides the NCCO samples, we prepared Nb and YBCO samples to obtain a clear comparison of the electrodynamic properties of different superconducting samples. Nb samples were prepared by cutting small pieces from a large pure Nb single crystal. The surface of each sample was mechanically polished, and then etched for a few seconds with a solution (HF 40% volume and 60% HNO_3 volume), and subsequently polished lightly with very fine alumina powder. After the surface treatment, each sample was cleaned with ethanol and then stored in a high vacuum chamber for a few days. Each Nb sample was examined with a high-resolution optical microscope,

which revealed that the sample surface has no damage and retains single-crystal grain structure. Furthermore, optical microscopy indicates that the surfaces are clean, smooth, and homogeneous, and do not show any discoloration.

YBCO crystals were grown by the flux motion in zirconia crucibles and subsequently annealed in flowing O_2 for several weeks, in a manner similar to that of Ref. 32. Typical crystal sizes for microwave measurements are $\sim 2 \times 0.75$ mm^2 with a thickness ~ 20 μm. Selected crystals have smooth surfaces and do not exhibit any flux residue on the surface. High-resolution (better than $\times 1000$ in magnification) polarized light microscopy shows a somewhat inhomogeneous density of microtwin structures, with the greatest density corresponding to twin bands approximately 0.3 μm wide. dc SQUID measurements of the crystals prior to microwave measurements show a single sharp transition with transition width δT_c (< 0.2 K) at the transition temperature T_c (= 92.0 K). Considering the applied field strength in the dc SQUID measurement (~ 10 Oe), the high transition temperature and the sharp transition width indicates that our YBCO single crystals are of reasonably high quality. In microwave measurements, these crystals show a single sharp transition at T_c (~ 92 K), hence we did not need to etch or modify the YBCO samples. Dc transport measurements on the crystals show that they have normal-state resistivities at 100 K on the order of 40 $\mu\Omega$ cm and $d\rho/dT = 0.5$ Ω/K,[33] substantially lower than those reported by the University of British Columbia (UBC) group for their crystals.[32] Further, we note that the transport properties (ρ_n and $d\rho/dT$) of our YBCO crystals are nearly identical to those of the Illinois group.[34]

EXPERIMENT

The complex surface impedance $Z_s(= R_s + iX_s)$ of the samples was measured in a cylindrical Nb superconducting cavity excited in the TE_{011} mode with the sample supported on a sapphire hot finger.[36,37] All samples were measured with H_{rf} parallel to the sample surface (i.e. for cuprates, $H_{rf} \| ab$ axis). The Nb cavity was thermally treated in a very high vacuum to recrystallize the surfaces and render a very high Q ($> 2.2 \times 10^7$) with resolution $\delta(1/Q) \sim 10^{-9}$ and stable resonant frequency ($\delta f/f < 1 \times 10^{-9}$) at the cavity operating temperature $T < 4.2$ K. The temperature of the hot finger was independently varied from below 4.2 to over 100 K, without substantial heating of the Nb cavity. With the temperature variation, the resonance frequency f and the quality factor Q of the cavity are measured. The temperature dependence of the surface impedance, Z_s (i.e., the surface resistance R_s and the reactance X_s, or the change of the penetration depth $\delta\lambda$) is extracted from the Q and the change in resonant frequency δf using the relations $R_s = \Gamma(1/Q - 1/Q_{cav})$, $\delta X_s = 2\pi f \mu_0 \delta\lambda$, and $\delta\lambda = -\zeta \delta f$.[35] Here Q_{cav} is the quality factor of cavity without sample, while Γ and ζ are the geometrical factors which depend on the resonant mode, the size of the cavity, and the sample size and shape.[36,37] To determine the geometrical factors, we performed both theoretical calcu-

lations and also careful experimental calibrations. In the calibrations, we used Nb samples of dimensions similar to the NCCO and YBCO samples and determined the geometrical factor for each sample experimentally. The geometrical factors obtained from the calibrations were close to those calculated from our knowledge of the cavity and sample geometry. Also the value determined for Γ was independently verified by comparing a measured microwave R_s in the normal state with a calculated $R_s[=\sqrt{\rho_n\omega\mu_0/2}]$ obtained from independent measurements of the dc resistivity[33] and our microwave measurement frequency.

To extract an exact and meaningful temperature dependence of R_s and λ from the raw data, one needs to account for the temperature dependence of the cavity background. Although the technique we have employed keeps the temperature-dependent background of the cavity and sapphire hot finger negligibly small at low temperatures (in our experiments $T < 30$ K), because of thermal radiation and the temperature dependent dielectric constant of the sapphire hot finger, there is a considerable temperature dependent background (i.e., Q_{cav} and the resonant frequency of the cavity) as we measure samples at higher temperatures. For NCCO and Nb samples, because their transition temperatures are so low and measurements are performed only over the temperature range 2 K $\leq T \leq 30$ K, these temperature-dependent background corrections were negligible, and do not limit the resolution for either R_s or λ. With a typical size of NCCO thin film sample $(3 \times 5$ mm$^2)$, we achieved a resolution in $R_s \sim 10$ $\mu\Omega$ and $\delta\lambda \leq 2$ Å. However, for YBCO, the temperature-dependent background significantly affects the determination of R_s and λ. For this reason, we measured the background precisely from 2 to 250 K before and after each measurement with a YBCO sample. Throughout the background measurements, we verified that the background data are highly reproducible. With typical YBCO single crystals with the dimension 2×0.75 mm^2 and 20 μm thick, we obtained a resolution for $R_s \sim 20$ $\mu\Omega$ and $\delta\lambda \sim 3.5$ Å which are precise enough to examine the temperature dependence of the electrodynamic parameters in the entire temperature range.

RESULTS

The experimental results obtained from NCCO and YBCO samples were first examined with no specific model for superconductivity in mind. Since it is widely believed that the symmetry of the pairing state of a superconductor is directly manifested in the low-temperature dependence of Z_s, we examined the raw data (i.e., Q and the resonance frequency) to learn about the electrodynamics of the samples with a minimum of assumptions and ambiguities. Because of the simple relation $R_s \propto 1/Q(T) - 1/Q_{cav}(T)$ and $\delta\lambda \propto \delta f(T)$, one can discern the temperature dependence of R_s and λ directly from the raw data. In this study, we measured many different samples with different sizes and shapes. Accordingly the geometrical factors are different for each of the samples we measured. Also additional complications may occur with thin films because the finite film thickness

alters the measured value of R_s and λ near T_c.[38] In order to avoid these problems, we scale our data to remove the geometrical factors, and examine the data at low temperatures where finite film thickness corrections are negligible.

Figure 2 shows the comparative low-temperature behavior of various samples: single crystals of Nb, NCCO, and YBCO, as well as an NCCO thin film. There are obvious similarities between the data from Nb and NCCO samples, and a dramatic difference between YBCO and the rest of the samples, in their temperature dependence. To obtain the best fit to the data, we have tried several possible functional forms suggested by phenomenology. Recent results on YBCO suggest fits of the form $\delta\lambda \sim T^n$, $aT + bT^2$ or the traditional exponential dependence, $\alpha T^{-1/2} \exp(-\beta/T)$. The values of n, a, and b, or α and β were adjusted to yield the best fit. For the frequency shift data on Nb and NCCO, the best fit can be obtained with the BCS s-wave type exponential, dependence, $\delta f \propto 1/\sqrt{T}\exp(-\Delta(0)/k_B T)$ with an activation barrier $2\Delta(0)/k_B T_c \approx 4.0$–4.2 for both Nb and NCCO. The other functional forms T^n and $aT + bT^2$, also can yield equally good fits to the data if $n \geq 4$ (which is, in practice, indistinguishable from the exponential) or if $a < 0$. For the latter case, however, we believe that the
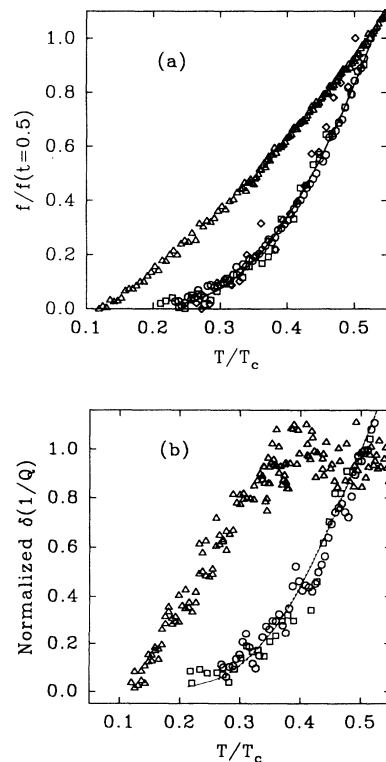
FIG. 2. (a) Normalized frequency shift and (b) quality factor data at low temperatures $T < T_c/2$ for an NCCO thin film on a buffered sapphire substrate (squares), an NCCO single crystal (diamonds), a Nb single crystal (circles), and a YBCO single crystal (triangles). Solid lines are a BCS s-wave fit to the Nb and NCCO data.

fitting form has no physical meaning unless $a \geq 0$. While the frequency shift data from Nb and NCCO suggest clear exponentially activated behavior in their temperature dependence, the data for YBCO are distinct, and are best described with a power-law temperature dependence $\delta f \propto T^n$ or $\delta f \propto aT + bT^2$ with both a and $b > 0$. Interestingly, if we choose the $\delta f \propto T^n$ dependence, we found that the value of the exponent varies depending on the temperature range. For example, if we choose the temperature range to be $0.12 < T/T_c < 0.89$, we obtain $n \sim 1.7$, whereas if the temperature range is $T/T_c < 0.2$, the exponent becomes $n \sim 1.2$.

For the data $\delta(1/Q(T)) = 1/Q - 1/Q_{cav}$, similar results were obtained from the fits, $\delta(1/Q(T)) \propto (1/T)\exp(-\Delta(0)/k_B T)$. The data from Nb and NCCO samples are consistent with the exponential behavior with the gap ratio $2\Delta(0)/k_B T_c \approx 4.0-4.2$, as well as the power-law dependence with $n \geq 4$. Hence, from the comparison with Nb and also from the fit, both the Q and f of NCCO strongly suggest the s-wave BCS-type temperature dependence of R_s and λ at low temperatures. For YBCO, however, the temperature dependence of $\delta(1/Q)$ shows a linear temperature dependence at very low temperatures and nonmonotonic behavior at higher temperatures, which is qualitatively consistent with the results obtained by Bonn and co-workers.[3,4] Hence we were not able to reconcile the low-temperature data from YBCO with any exponential temperature dependence.
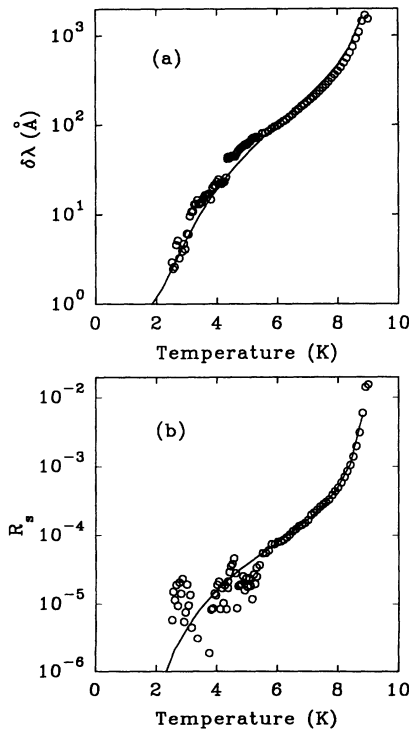
The similarities and contrasts among these samples are very intriguing, and we would like to make further detailed analysis and comparisons over the entire temperature range. For quantitative analysis and comparison, we convert δf and Q into $\delta\lambda$ and R_s. Since our data from Nb show the standard BCS s-wave behavior, and its properties for pure single crystals have been well understood,[39] we first examine the data from Nb to verify the geometrical factor and demonstrate the legitimacy of subtracting a residual resistance from the data. The temperature dependence of the penetration depth $\delta\lambda(T)$ and the surface resistance $R_s(T)$ of Nb exhibit a typical BCS s-wave behavior as shown in Fig. 3. The BCS fits yield $\lambda_{eff}(0) \sim 400$ Å, $l_{mfp} = 450$ Å, and $\xi_0 = 760$ Å. Using these three quantities we can deduce the London penetration depth from $\lambda_{eff} = \lambda_L \sqrt{1 + \xi_0/J(R=0,T)l}$, and we obtain $\lambda_L = 320$ Å, which is close to the value of $\lambda_L = 315$ Å found by magnetization.[40] The fit also yields $R_s(T_c) \sim 12$ mΩ, which is within 20% of the calculated value, $R_s(T_c) = \sqrt{\rho_n(T_c)\omega\mu_0/2}$, and reflects the maximum of our experimental uncertainty. This verifies that calculated geometrical factors and our conversion process used in this work are acceptable within reasonable limits of error.

NCCO PENETRATION DEPTH

For NCCO samples, in particular the new thin films, we found that the BCS s-wave like features continue up to near T_c, in agreement with our earlier results.[20] As shown in Fig. 4, a clear quantitative agreement with a calculation based on the BCS s-wave model can be found within the temperature range 4 K $< T < 20.5$ K. The BCS numerical calculation was performed using a computer code described by Halbritter.[41,42] The calculation requires several input parameters, including a measurement frequency f, transition temperature T_c, the London penetration depth λ_L, the coherence length ξ, the quasiparticle mean free path l, and gap ratio $2\Delta(0)/k_B T_c$. Among those parameters, f, T_c, and ξ were determined

FIG. 3. (a) Change in magnetic penetration depth $\delta\lambda(T)$, (b) and change in surface resistance $\delta R_s(T)$ for a Nb single crystal. Solid line is the s-wave BCS calculation discussed in the text.
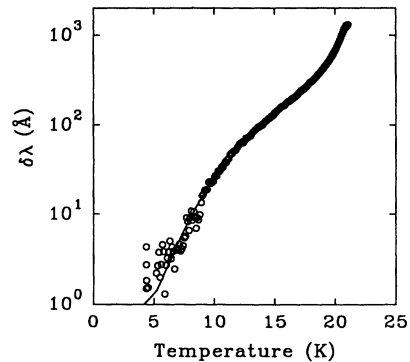
FIG. 4. Change in magnetic penetration depth, $\delta\lambda(T)$, for an NCCO thin film on a buffered sapphire substrate. The solid line is the s-wave BCS calculation discussed in the text. The data have not been corrected for finite thickness, although the theory has been (Ref. 38).

by independent experiments. The London penetration depth λ_L and mean free path l were determined with some experimental guidance, as the experimentally determined effective penetration depth λ_{eff} constrains λ_L through $\lambda_{\text{eff}} = \lambda_L \sqrt{1 + \xi_0/J(R=0,T)l}$. The gap ratio was used as the only completely free parameter. Also the interplay between λ_L and $\Delta(0)/k_B T_c$ could change the value of λ_L as $\Delta(0)/k_B T_c$ varies. Generally, to obtain a reasonable fit to our data, one must reduce the value of λ_L as the gap ratio increases.

The effective in-plane penetration depth $\lambda_{\parallel}^{\text{eff}}(0)$ is deduced from a plot $d\lambda_{\parallel}/dy$ vs $y \equiv 1/(1-t^4)^{1/2}$, as shown in Fig. 5 Note that the value of $d\lambda_{\parallel}/dy$ for $y > 2$ converges to yield $\lambda_{\parallel}^{\text{eff}}(0) \sim 760 \pm 50$ Å. Using the value $\xi_0 \sim 80$ Å and $l \sim 650$ Å, we deduce $\lambda_{L\parallel} \sim 720 \pm 50$ Å. These values, along with a choice of gap ratio $2\Delta/k_B T_c = 4.06 \pm 0.1$, yield the best fit for our experimental $\lambda_{\parallel}(T)$ data. We also note that in Fig. 5, $d\lambda_{\parallel}/dy$ diverges for $y < 1.3$, similar to what has been seen in typical BCS superconductors as evidence of a finite energy gap in the low-lying excitation spectrum of the superconductor.[43,44] It is important to note that the divergence in $d\lambda_{\parallel}/dy$ observed from our samples is not a spurious effect due to existence of other superconducting phases, as was seen in a defective Nb sample.[45] Other temperature dependences, like $\lambda(T) = \lambda(0)/\sqrt{1-(T/T_c)^n}$, with $n = 1$ or 2, also diverge at low temperatures when plotted in this way. However, the inset in Fig. 5 shows that the BCS s-wave temperature dependence with the gap ratio $2\Delta(0)/k_B T_c = 4.06$ (corresponding to $\Delta(0) \approx 3.67$ meV) shows the best resemblance to our data. This value of the energy gap is also in good agreement with the tunneling results (obtained by a point-contact method) on a NCCO sample by Huang *et al.*,[46] and is also consistent with a gap value suggested by the exponential dependence of the raw $f(T)$ and $Q(T)$ data mentioned previously. Finally we would like to point out that from the BCS fits, the gap value is not only valid at low temperatures, but is also

valid over the whole temperature range, which strongly suggests a single gap s-wave behavior throughout the entire temperature range. It has recently come to our attention that microwave measurements on NCCO films made at IBM have largely confirmed our main results for the penetration depth temperature dependence.[47]

NCCO SURFACE RESISTANCE

The surface resistance $R_s(T)$, converted from $Q(T)$, also validated the electrodynamic properties which have been identified from $\lambda(T)$. The behavior of R_s with temperature for a thin film is shown in Fig. 6, which compares the data with the BCS s-wave calculation. A quantitative agreement between the experimental R_s^{exp} and the theoretical R_s (solid line in the main figure) can be obtained if we use slightly modified parameter values from those for $\lambda(T)$. We further use a modified relation $A^* R_s = R_s^{\text{exp}} - R_0$, where A^* is a correction factor, and R_0 is the temperature-independent residual resistance, as is commonly done for conventional superconductors. For example, Turnaeure and co-workers have made a very detailed comparison between the BCS s-wave theory and their experimental data on bulk niobium.[39,42] They obtained a residual resistance of 2×10^{-8} Ω at 11.2 GHz,

FIG. 5. Plot of $d\lambda/dy$ vs $y \equiv 1/[1-(T/T_c)^4]^{1/2}$ for an NCCO thin film on a buffered sapphire substrate. Solid line is the BCS calculation. Dashed line is obtained from $\lambda(T) = \lambda(0)/[1-(T/T_c)^2]^{1/2}$, and dotted line from $\lambda(T) = \lambda(0)/[1-(T/T_c)]^{1/2}$. The inset shows the low-temperature data in greater detail.
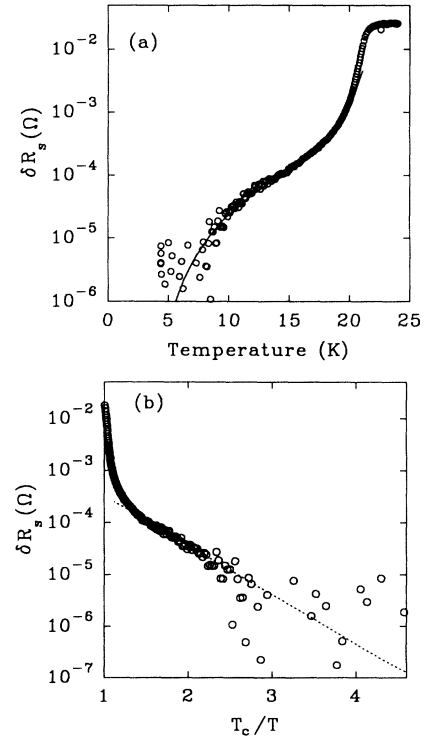
FIG. 6. Change in surface resistance $\delta R_s(T)$ of an NCCO thin film on a buffered sapphire substrate, (a) shows $\ln \delta R_s(T)$ vs temperature, while (b) shows the same vs T_c/T, emphasizing the low temperature data. The solid line in (a) is the BCS calculation, while the dashed line in (b) indicates the exponential behavior $R_s \propto e^{-\Delta(0)/k_B T}$ at low temperature. The data have not been corrected for finite film thickness, although the theory has been (Ref. 38).

with a correction factor $A^* = 0.97 \pm 0.02$. To our knowledge, their work is regarded as the most detailed and thorough comparison of a conventional superconductor with the BCS s-wave model. We note that the value of the correction factor is closely related with the choice of the parameter values used in the fit. Considering these, our correction factor $A^* \approx 1.1-1.35$ implies that the parameter values used in this work are reasonable.

The residual resistance of our earlier films on $LaAlO_3$ was large: on the order of 2.5 mΩ at 4.2 K and 9.6 GHz. These high values raised many questions about our previous results on the electrodynamic properties of NCCO. The situation has been dramatically improved as we have successfully fabricated new and better thin films.[28,29] The new thin films on buffered sapphire show substantially lower residual resistances, $R_s(0) \sim 80$ $\mu\Omega$ at 4.2 K and 9.6 GHz. Comparing these results to those on NCCO/$LaAlO_3$, we are forced to conclude that the large residual resistances of the earlier films are not due to a d-wave-like pairing state, as may have been argued by some investigators. Instead we believe that the higher residual resistances in the earlier films reflect the degree of material imperfection of those films.[28]

Another interesting observation was that although the $R_s(T)$ data in general display good agreement with the calculation over a very broad temperature range, a slight disagreement can be found near T_c, where a simple two-fluid-like dependence $R_s \sim \lambda(T)^3(T/T_c)^4$ better fits the experimental data. Such a disagreement may occur for many reasons. In part, this indicates that a considerable number of unpaired charge carriers or quasiparticles exist at temperatures near T_c, and R_s is much more sensitive to the existence of the unpaired charge carriers than λ. Another possible reason is due to an improper choice of the parameter values in the numerical calculation. Although we have tried to fit the R_s data with the calcula-

tion by choosing the parameter values as well as possible, we found that the calculated R_s is much more sensitive to the choice of the parameter values than λ.

Interestingly, such disagreement is less pronounced for the new films. This suggests that the material imperfection influences not only the residual resistance but also the quasiparticle dynamics. Nevertheless, what is significant is the remarkable agreement over orders of magnitude between the experimental surface resistance R_s^{exp} and the single-gap BCS calculation in the entire temperature range. We also emphasize that our results clearly show the exponential behavior $R_s \propto e^{-\Delta(0)/k_B T}$ at low temperatures as indicated by the dashed line in Fig. 6(b).

We found that the electrodynamic parameter values used in the numerical calculations for the new thin films are very similar to those of the earlier thin films. Table I displays a summary of the electrodynamic parameter values used in the BCS numerical calculation for both R_s and λ. With these values, in general, we were able to obtain reasonable and reproducible fits to both $R_s(T)$ and $\lambda(T)$ obtained from several NCCO samples.

POWER DEPENDENCE OF NCCO

Besides the temperature dependence of λ and R_s, one also can explore the pairing state of a superconductor from its magnetic-field dependence of λ and R_s. In this study, we attempted to probe the pairing state of NCCO with the variation of the microwave field strength. In our earlier study, preliminary results on the microwave field dependence of λ and R_s were obtained near T_c.[20] The data could be represented with a quadratic field dependence as $\delta R_s(H_{rf}) \equiv R_s(H_{rf}) - R_s(0) = g(T)H_{rf}^2$, where $R_s(0)$ is the surface resistance at nearly zero field, $g(T)$ is an experimentally determined coefficient and H_{rf} is the microwave magnetic-field strength parallel to the sample surface. This quadratic dependence on field strength was understood as a typical signature for a BCS s-wave superconductor when the sample is in the Meissner state $(H_{rf} < H_{c1})$.

We have further explored the field dependence over a broad temperature range $(4.2 \text{ K} < T < 21 \text{ K})$ with both new and old samples. Near T_c, the quadratic dependence on H_{rf} was reproduced in all films. However, at low temperatures the results are better described by a field dependence which shows a monotonic change in power-law from quadratic to linear and then to sublinear field dependences as the temperature decreases. Typical field dependences at different temperatures are shown in Fig. 7. The behavior is not expected from a BCS s-wave material, and the origin of the anomalous field dependence is not yet clearly understood. A linear increase of both R_s and λ with H_{rf} has been seen before in NbN and YBCO thin films,[48] where it was ascribed to weak links in those films. Magnetic-flux entry at weak links is also a possibility with the present films, as well as the response of trapped magnetic flux in our samples. Also one may suggest that the anomalous field dependence might occur due to the existence of other superconducting phases in our thin films. However, we are forced to rule out such a

TABLE I. Electrodynamic parameters used to fit the $\lambda_\parallel(T)$ and $R_s(T)$ data with the BCS calculation for $Nd_{1.85}Ce_{0.15}CuO_4$. Parameters above the center line were determined by independent means, and those below the line were used as fitting parameters.

Property	Thin films on $LaAlO_3$	Thin films on Al_2O_3	Single crystal
T_c (K)	21	21.5	21.5
$\lambda_\parallel(0)$ (Å)	1300±100	760±50	1250±200
$\xi_\parallel(0)$ (Å)	72–80	80	80
R_0 (mΩ) at 9.6 GHz	2.5	0.08	1
l_{MFP} (Å)	115–660[a]	650[b]	300±200
$2\Delta(0)/k_B T_c$	4–4.3	4.06±0.1	3.9–4.3
$\lambda_{L\parallel}$ (Å)	1000±90	720±50	1050±200

[a]For the NCCO films on $LaAlO_3$ substrate, we used $\xi_\parallel(0) \sim 72$ Å and $l \sim 600$ Å for $R_s(T)$, and $\xi_\parallel(0) \sim 80$ Å and $l \sim 115$ Å for $\lambda_\parallel(T)$ to obtain the best fit.

[b]For the new NCCO films on sapphire substrates, we used $\xi_\parallel(0) \sim 80$ Å and $l \sim 650$ Å for both $R_s(T)$ and $\lambda_\parallel(T)$.
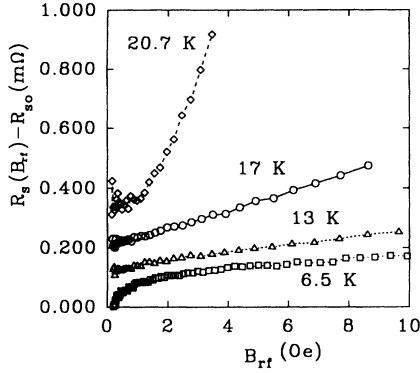
FIG. 7. Change in surface resistance $\delta R_s(H_{rf})$ vs rf field strength at various temperatures in an NCCO thin film. Note that typical field dependence changes from quadratic to linear and then linear to sublinear as the sample temperature decreases. R_{s0} is chosen arbitrarily for each temperature to offset the data for clarity.

possibility because our results from $\lambda(T)$ and $R_s(T)$ exclude the existence of other superconducting phases in our NCCO thin films. Detailed comparison with other materials and theoretical interpretation on the anomalous field dependence are underway.

NCCO DISCUSSION

Our results on NCCO indicate that the temperature dependence of R_s and λ of NCCO is strikingly similar to those of the BCS s-wave superconductors. Our observations of the temperature dependence of R_s and λ are unprecedented for the cuprate superconductors. We know of no other instance in which (a) cuprate superconductors show activated behavior of the surface impedance over such large barriers, (b) there is such close agreement between the temperature dependences of R_s and λ at low temperatures in the same sample, and (c) there is such close agreement between thin film and single-crystal samples of the same material. These unique observations argue forcefully that we are either examining the intrinsic electrodynamic response of NCCO, or alternatively, an extrinsic phenomenon inherent to thin films and single crystals which affect the condensate and quasiparticles in the same way.

PENETRATION DEPTH OF YBCO

The penetration depth $\lambda(T)$ of YBCO is presented in Fig. 8. We believe that the data are dominated by screening currents in the ab plane of YBCO. Although very near T_c the data can be described either by the simple two fluid model or by the BCS s-wave model, a clear deviation from the BCS s-wave or two-fluid model is obvious at low temperatures. As mentioned earlier, the low-temperature data are better described by a power law $\delta\lambda(T) \propto T^n$ with $1.2 \leq n \leq 1.7$, depending on the choice of temperature range. At low temperatures, the power-law dependence is similar to what Hardy *et al.* have reported,[1] while over a broader temperature range it is closer to
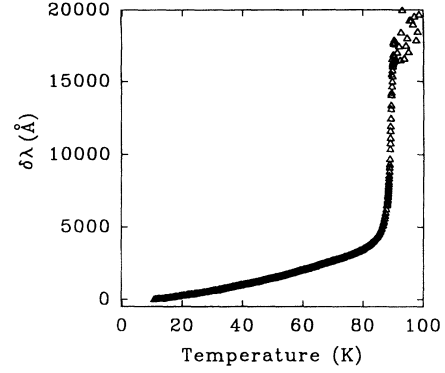
FIG. 8. Change in magnetic penetration depth $\delta\lambda(T)$ for a YBCO single crystal, showing near linearity with temperature below 80 K.

a quadratic temperature dependence. To furnish a more detailed comparison between our data and others, we plot $d\lambda/dy$ vs y in Fig. 9. Our data show that the value of $d\lambda/dy$ converges to ~ 1450 Å at high temperatures where $y > 2$. The value is consistent with the effective penetration depth at zero temperature reported earlier by muon-spin rotation measurements.[4] However, the YBCO data show that $d\lambda/dy$ diverges rapidly even at moderate temperatures where $y < 2$, in strong contrast with the conventional behavior of the BCS s-wave superconductors. This is obvious from the comparison of Fig. 5 and Fig. 9. We found our $\lambda(T)$ is better described by a simple combination of power laws, either $a + bT + gT^2$ or $a + bT^n$ with a temperature dependent n.

YBCO SURFACE RESISTANCE

After extracting the surface resistance $R_s(T)$ from $Q(T)$, we compared $R_s(T)$ in the normal state with $R_n = \sqrt{\rho_n(T)\omega\mu_0/2}$ to confirm the validity of our conversion process. The results are very consistent in the normal state and hence confirm that our converted $R_s(T)$ is valid. In Fig. 10, we present $R_s(T)$ for the YBCO crys-
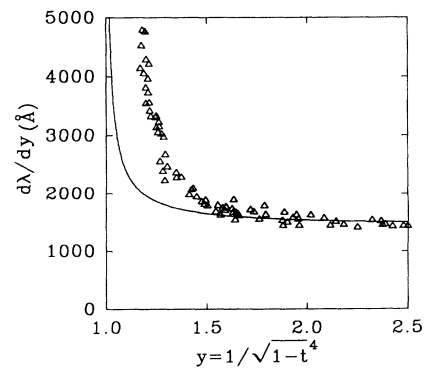
FIG. 9. $d\lambda/dy$ vs $y \equiv 1/[1-(T/T_c)^4]^{1/2}$ for a YBCO single crystal. Solid line is $d\lambda/dy$ from $\lambda(T) = \lambda(0)/[1-(T/T_c)]^{1/2}$ discussed in the text. From the high-temperature limit, one finds $\lambda_{eff}(0) \sim 1450 \pm 50$ Å.
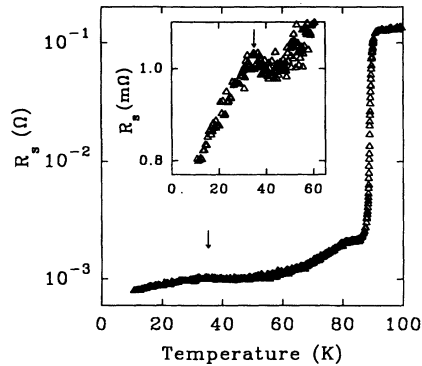
FIG. 10. Change in surface resistance $\log_{10}\delta R_s(T)$ vs temperature in a YBCO single crystal. The inset shows a linear plot of $\delta R_s(T)$ showing the nonmonotonic temperature dependence and a peak at approximately 35 K.

tal. The figure shows that $R_s(T)$ drops rapidly below T_c and has a broad low peak at $T \sim 35$ K. Moreover, the surface resistance shows roughly a linear temperature dependence below 20 K. Hence, the data indicate the temperature dependence of R_s from YBCO is also anomalous. The results are similar to what Bonn and co-workers have observed from their YBCO samples.[3,4] Although all of these observations are in qualitative agreement with theirs, we find that there are several quantitative inconsistencies. First of all, the residual surface resistance (~ 750 $\mu\Omega$ at 9.6 GHz) in our data is more than three times larger than their residual surface resistance (~ 200 $\mu\Omega$, when scaled to 10 GHz by ω^2) measured on twinned crystals, while the dc resistivity at 100 K of our sample (~ 40 $\mu\Omega$ cm) is almost half of theirs (~ 72 $\mu\Omega$ cm).[32] Our crystals also show a hint of nonlinearity in $\rho_n(T)$ between 100 and 300 K. Also we note that our $R_s(T)$ data show a small foot just below T_c which was absent or perhaps negligibly small in the data of Bonn et al.[3] We believe some of these inconsistencies are probably due to sample imperfection in our YBCO crystals, possibly oxygen inhomogeneity or oxygen over-doping. Further results on these YBCO crystals will be presented in future publications.[49]

YBCO DISCUSSION

With YBCO single crystals, the data clearly exhibits that the temperature dependence of $R_s(T)$ in nonmonotonic with a broad peak at around $T \sim 35$ K and linear for $T < 20$ K. Also the tendency for an almost linear change of $\lambda(T)$ at low temperatures is obviously not consistent with a BCS s-wave model. Rather, these observations are more likely consistent with results obtained by Bonn et al. This demonstrates that our sample preparation and measurement techniques can produce YBCO samples showing clear non-s-wave behavior. This makes our results on NCCO much more puzzling, because the preparation and measurement techniques for YBCO and NCCO are nearly identical.

GENERAL DISCUSSION

In this work, we have examined the electrodynamic properties of Nb, NCCO, and YBCO. These represent a conventional three-dimensional BCS s-wave superconductor, an electron-doped cuprate, and a hole-doped cuprate superconductor. Among cuprates, in principle, NCCO should be one of the simplest and most easily understood examples of cuprate superconductivity. While the material shares the general cuprate properties, it has single Cu-O plane layers, tetragonal crystal structure at the optimum superconducting doping, and relatively long in-plane coherence length. In contrast to NCCO, YBCO has a second kind of conducting Cu-O layer in the crystal structure and suffers from heavy twinning because of its orthorhombic structure. Moreover, YBCO has a short in-plane coherence length, making many electrodynamic properties subject to modification by weak-link effects.

It is important to note that NCCO shares a number of important physical properties with the hole-doped cuprates. They are all antiferromagnetic insulators in the limit of low doping, although the antiferromagnetic state persists to higher doping in NCCO than in the hole-doped cuprates.[50-52] There is ample evidence that strong inelastic scattering takes place in the normal state of both electron- and hole-doped cuprates, particularly from far-infrared reflectivity measurements. These results suggest that the excitations which cause scattering in the normal state are the same for both hole- and electron-doped materials.

Despite the similarities of many important physical properties, during this work we found that there are noticeable differences between the electrodynamic properties of NCCO and YBCO in the superconducting state. This brings up a very important and fundamental question: To what extent do our observation on NCCO and YBCO reflect their intrinsic nature? If our observations reflect mostly the intrinsic properties of each sample, what causes the differences in the same cuprate family? If there are some extrinsic effects, why are they so consistent between films and crystals of NCCO, and so inconsistent between films and crystals of YBCO?

Some key physical properties of the NCCO and YBCO materials are contrasted in Table II. Among many differences between the two materials, the most noticeable difference is the fact that YBCO is an ordered, stoichiometric compound at optimal doping, whereas NCCO is thought to be a random alloy due to the disordered Ce doping on Nd sites. In addition, for both cuprates, there is disorder on the oxygen sites, as suggested by a great deal of work on the YBCO Cu-O chains, and by electron microscopy on NCCO.[53] It may be that due to its more disordered nature, NCCO shows a nonlinear normal-state resistivity $[\rho_n(T) \sim T^2]$ with signs of a constant residual resistivity setting in above T_c.[54] Magnetoresistance measurements by Kussmaul[55] and Hagen et al.[56] also show that the underdoped NCCO material shows evidence of weak localization of the charge carriers. From transport measurements, Jiang et al. have shown that excess oxygen in as-prepared NCCO crystals may cause localization of the electrons introduced by Ce

TABLE II. Contrasting physical properties of $YBa_2Cu_3O_7$ and $Nd_{1.85}Ce_{0.15}CuO_4$.

Property	$YBa_2Cu_3O_7$	$Nd_{1.85}Ce_{0.15}CuO_4$
Crystal structure at maximum T_c	Orthorhombic	Tetragonal
Conducting layers in unit cell	Double CuO_2, Cu-O chain layer	Single CuO_2, no chains
Apical oxygens	Distorted but occupied	Nominally unoccupied
"Order"	"Stoichiometric compound"	"Random alloy"
T_c	~92 K	~22 K
Coherence length		
In-plane	$\xi_{ab} \sim 10$–15 Å	$\xi_a \sim 70$–80 Å
c direction	$\xi_c \sim 2$–5 Å	$\xi_c \sim 15$ Å (Ref. 66)
Mass anisotropy	6	21 (Ref. 66)
m_c/m_{ab}		25 (Ref. 58)
Sign of carriers:		
Nominal doping	Holes	Electrons
Hall effect (at max T_c)	Holes	Electrons (Ref. 66)
Thermopower	Holes (except for $YBCO_{7.0}$)	Holes (Ref. 67)
Photoemission FS	Holes	Holes (Ref. 63)
Normal state:		
Resistance	$\sim T$	$\sim T^2$
Scattering rate	$\sim \omega$	$\sim \omega$ (Ref. 68)
Hall angle: $\cot\theta_H$	$\sim T^2$	$\sim T^4$

doping.[57] We speculate that poor oxygen stoichiometry, or the random doping of Ce, may be responsible for the observation of weak localization. Finally, the higher RBS channeling yields in NCCO films also suggest a greater density of point defects. To summarize, several types of data all suggest that NCCO is a more disordered material than its hole-doped brethren.

To our knowledge the differences in electronic structure of cuprates between electron and hole doping have not been explored in detail. Starting from an antiferromagnetic insulator and doping with holes is thought to increase the magnetic frustration in the copper-oxygen planes and quickly extinguish long-range antiferromagnetic order.[58] Electron doping, on the other hand, is thought to simply dilute the spin system in the copper-oxygen planes, allowing for persistence of antiferromagnetic correlations to much higher doping levels. Whether these correlations still exert some influence in the superconducting state is not known, but the asymmetry is clearly important. Whether or not this asymmetry has an effect on the symmetry of the ground-state superconducting wave function is not known either. However, Rokhsar proposes that electron doping a Mott insulator will lead to s-wave pairing in the superconducting state, while hole doping eventually leads to d-wave pairing.[59]

Recently some theoretical proposals have been made to explain our experimental results on NCCO. Lee has suggested that the electrodynamic properties of d-wave superconductors will be very sensitive to the presence of disorder due to strong (unitary limit) scatterers, and that a disordered d-wave superconductor will develop a "mobility gap" near the nodes of the d-wave energy gap.[12] Below this mobility gap, the low-lying quasiparticle states will become localized on relatively short length scales and effectively no longer participate in transport processes. An energy scale Δw is the typical energy level spacing be-

tween states within a localization length of each other. Lee estimates that $\Delta w \sim \gamma_0 (\Delta_0/\varepsilon_F) e^{-2\varepsilon_F/\Delta_0}$, where $\gamma_0 = \Delta_0/(\Delta_0\tau)^{1/2} \sim \Delta_0$, Δ_0 is the maximum gap on the Fermi surface, and ε_F is the Fermi energy.[12] The surface resistance, and possibly the penetration depth as well, will be affected by this localization, and show a disorder-induced artificial energy gap in their low-temperature transport properties $(k_B T < \Delta w)$. According to this picture, the measured energy gap in NCCO will be very sensitive to the type and extent of disorder in the thin films and single crystals. From Lee's estimate above, using $2\Delta_0/k_B T_c \sim 4$, and $\Delta_0\tau \sim 1$, we find that $2\Delta w/k_B T_c \sim 0.5$.[12] However, this gap is substantially smaller than those deduced from our microwave surface impedance data at low temperatures.

Furthermore, several experimental observations would seem to be at odds with the mobility gap idea. First is our observation of very nearly the same activated temperature dependence of λ and R_s in both thin films and single crystals. It is commonly believed that the nature of disorder is entirely different in thin films and single crystals. The thermodynamic and kinetic conditions present during growth of a thin film and crystal are very different, and arguments hinging on this difference have been made before to explain the high residual losses in twinned YBCO crystals as compared to YBCO films.[16] Hence we find it difficult to believe that the same disorder-induced mobility gaps would develop in our films and crystals of NCCO.

A second experimental observation at odds with the mobility gap idea is the work of Klein and co-workers on the oxygen dependence of the surface resistance in YBCO thin films.[17,60] They found that the residual surface resistance decreased with longer annealing times in activated oxygen. At the same time, the activation energy for

ELECTRODYNAMICS OF $Nd_{1.85}Ce_{0.15}CuO_4$: COMPARISON . . .

$R_s(T)$ at low temperatures increased with prolonged annealing. Klein and co-workers suggest that the annealing resulted in an increase in the oxygen content of the film and a decrease in the disorder of the oxygen chain sublattice. These results suggest that decreasing disorder among the oxygen in YBCO actually serve to increase the activation barrier, quite the opposite from what is expected of a mobility gap.

The electrodynamic properties of d-wave superconductors have been calculated in detail by Hirschfeld and co-workers.[13,15] They find that very clean d-wave superconductors have a pure limit response in which the magnetic penetration depth increases linearly with temperature: $\lambda(T)=\lambda_L+c_1T$, where λ_L is the London penetration depth, and $c_1 \sim \ln2\lambda_L/(\Delta_0/k_B)$, and Δ_0 is the maximum of the gap function of the Fermi surface. Below a characteristic temperature T^* (which depends on the degree of disorder) a disorder-dominated limit is reached in which the penetration depth increases quadratically with temperature: $\lambda(T)=\lambda_0+c_2T^2$. The coefficient $c_2 \sim n_i^{-1/2}$, where n_i is the density of resonant (unitary limit) scattering sites. In addition, $T^* \sim n_i^{1/2}$, so the disorder dominated temperature range expands to ever higher temperatures with increasing disorder. From fits to our penetration depth data of the form $\lambda(T)=\lambda_0+aT^2/(T^*+T)$, for $T<T_c/2$, we find that YBCO crystals have a $T^* \sim 10$ K. Our NCCO films and crystals show no sign of a linear temperature dependence in $\lambda(T)$, presumably because the density of resonant scatterers has pushed T^* above $T_c/2$. Note that increased disorder tends to decrease c_2, making the penetration depth temperature dependence look flatter at low temperatures. Hence in this d-wave picture, the only explanation for our NCCO results is a large degree of resonant scattering which has pushed $T^* \geq 20$ K without significantly decreasing T_c. However, the $\lambda(T)$ data for NCCO are still poorly fit by $\lambda(T) \sim aT^2$, suggesting that the simple approach of Hirschfeld et $al.$ does not apply to an extremely disordered material like NCCO, or that NCCO is not a d-wave superconductor. From all of the these observations we conclude that it is not possible to reconcile the NCCO data with the disordered d-wave electrodynamics calculations of Lee and Hirschfeld.

Other theoretical proposals of superconductivity in NCCO are based on phonon-mediated mechanisms of superconductivity. Point-contact tunneling spectroscopy measurements on NCCO by Huang et $al.$ showed a low zero-bias conductance, much lower than is ordinarily found for the hole-doped cuprates.[46] They were able to extract the $\alpha^2F(\omega)$ Eliashberg function from the d^2I/dV^2 data by conventional techniques. The $\alpha^2F(\omega)$ data bear some resemblance to the phonon density of states as obtained from inelastic neutron scattering.[52,61] They could calculate T_c in the context of Eliashberg theory, and found close agreement with the experimental T_c. Chen and Callaway have also calculated the T_c of NCCO based on strong-coupling theory and the Eliashberg equations, and also found fairly satisfactory agreement with the experimental T_c.[62]

Electron-phonon coupling in quasi-two-dimensional electronic systems with a van Hove singularity in the electronic density of states (DOS) have also been proposed to explain cuprate superconductivity. The T_c of such a system is very sensitive to the doping level because of the strongly peaked electronic DOS near the saddle point of the energy versus momentum relation. Relatively flat bands have been identified in the vicinity of the Fermi surface of our NCCO crystals by angle-resolved photoemission.[63] In this picture, the reason NCCO has such a low T_c is because its Fermi energy for the optimally doped material is well off the peak of the electronic DOS. In this situation, it has been observed that the normal-state scattering rate will increase as $T^2\ln T$, rather than as T, for the optimally doped material.[64] In addition, others have calculated the temperature dependence of the superconducting energy gap for a van Hove superconductor, and find, at most, a 5% deviation from the weakly coupled BCS temperature dependence,[65] consistent with our measurements of $\lambda(T)$ in NCCO. From these observations and calculations, it seems plausible that NCCO could be an electron-phonon-coupled s-wave superconductor. However, the role of antiferromagnetism in the copper-oxygen planes, and the details of the coupling mechanism, are far from being understood.

With our current experimental data alone, we cannot prove or disprove a particular theoretical model for the mechanism of superconductivity in NCCO. However, as our data suggest, we propose that a theoretical model for cuprate superconductivity should be able to explain why the electrodynamic properties of NCCO should and YBCO appear to be so different, and how these properties depend on disorder.

CONCLUSIONS

Our microwave surface impedance experiments reveal that the temperature dependence of R_s and λ from NCCO are strongly dissimilar to those of YBCO. Rather, they are in close quantitative agreement with the conventional BCS s-wave behavior. The reproducible activated behavior seen in the different sets of films, and in single crystals, strongly suggests that they are manifestations of intrinsic, or alternatively, highly reproducible extrinsic, phenomena. Interestingly, while some electrodynamic and tunneling data are all consistent with a traditional phonon-mediated s-wave pairing state in this material, our experimental results from the field dependence of R_s and λ do not yield a consistent BCS s-wave picture and hence suggest some possible nontraditional pairing state of the material. Also we found that it is difficult to reconcile the NCCO data with current calculations within the disordered d-wave picture.

[1]W. N. Hardy, D. A. Bonn, D. C. Morgan, R. Liang, and K. Zhang, Phys. Rev. Lett. **70**, 3999 (1993).

[2]Z. X. Shen, D. S. Dessau, B. O. Wells, D. M. King, W. E. Spicer, A. J. Arko, D. Marshall, L. W. Lombardo, A. Kapitulnik, P. Dickinson, S. Doniach, J. DiCarlo, A. G. Loeser, and C. H. Park, Phys. Rev. Lett. **70**, 1553 (1993).

[3]D. A. Bonn, P. Dosanjh, R. Liang, and W. N. Hardy, Phys. Rev. Lett. **68**, 2390 (1992).

[4]D. A. Bonn, R. Liang, T. M. Riseman, D. J. Baar, D. C. Morgan, K. Zhang, P. Dosanjh, T. L. Duty, A. MacFarlane, G. D. Morris, J. H. Brewer, W. N Hardy, C. Kallin, and A. J. Berlinsky, Phys. Rev. B **47**, 11 314 (1993).

[5]S. S. Laderman, R. C. Taber, R. D. Jacowitz, J. L. Moll, C. B. Eom, T. L. Hylton, A. F. Marshall, T. H. Geballe, and M. R. Beasley, Phys. Rev. B **43**, 2922 (1991).

[6]H. Piel and G. Müller, IEEE Trans. Magn. **27**, 854 (1991).

[7]A. T. Fiory, A. F. Hebard, P. M. Mankiewich, and R. E. Howard, Phys. Rev. Lett. **61**, 1419 (1988); J. Annett, N. Goldenfeld, and S. R. Renn, Phys. Rev. B **43**, 2778 (1991).

[8]S. M. Anlage, B. W. Langley, G. Deutscher, J. Halbritter, and M. R. Beasley, Phys. Rev. B **44**, 9764 (1991); J. F. Annett and N. Goldenfeld, J. Low Temp. Phys. **89**, 197 (1992); J. Stewart and N. Goldenfeld (private communication). See also Ref. 4.

[9]J. M. Pond, K. R. Carroll, J. S. Horowitz, D. B. Chrisey, M. S. Osofsky, and V. C. Cestone, Appl. Phys. Lett. **59**, 3033 (1991).

[10]M. R. Beasley, Physica C **209**, 43 (1993).

[11]Z. Ma, R. C. Taber, L. W. Lombardo, A. Kapitulnik, M. R. Beasley, P. Merchant, C. B. Eom, S. Y. Hou, and J. M. Phillips, Phys. Rev. Lett. **71**, 781 (1993).

[12]P. A. Lee, Phys. Rev. Lett. **71**, 1887 (1993).

[13]P. J. Hirschfeld, W. O. Putikka, and D. J. Scalapino, Phys. Rev. Lett. **71**, 3705 (1993).

[14]S. M. Anlage *et al.*, in *Oxide Superconductor Physics and Nano-Engineering*, edited by Davor Pavuna, SPIE Proc. Vol. 2158 (SPIE, Bellingham, WA, 1994), p. 94.

[15]P. J. Hirschfeld and N. Goldenfeld, Phys. Rev. B **48**, 4219 (1993).

[16]K. Zhang, D. A. Bonn, R. Liang, D. J. Baar, and W. N. Hardy, Appl. Phys. Lett. **62**, 3019 (1993).

[17]N. Klein, N. Tellmann, H. Schulz, K. Urban, S. A. Wolf, and V. Z. Kresin, Phys. Rev. Lett. **71**, 3355 (1993).

[18]E. R. Ulm, J. T. Kim, and T. R. Lemberger (unpublished).

[19]J. Halbritter, J. Appl. Phys. **68**, 6315 (1990).

[20]Dong-Ho Wu, Jian Mao, S. N. Mao, J. L. Peng, X. X. Xi, T. Venkatesan, R. L. Greene, and S. M. Anlage, Phys. Rev. Lett. **70**, 85 (1993).

[21]J. L. Peng, Z. Y. Li, and R. L. Greene, Physica C **177**, 79 (1991).

[22]D. P. Beesabathina, L. Salamanca-Riba, J. L. Peng, Z. Y. Li, and R. L. Greene, Physica C **208**, 79 (1993).

[23]A. R. Drews, M. S. Osofsky, H. A. Hoff, J. L. Peng, Z. Y. Li, R. L. Greene, and T. A. Vanderah, Physica C **200**, 122 (1992).

[24]The normal-state resistivity of the etched NCCO crystals $(\rho_n \sim 100 \ \mu\Omega \ \text{cm})$ is consistent with the experimental value of microwave surface resistance $R_n = (\mu_0 \omega \rho_n /2)^{1/2}$ of the single crystal within 10%.

[25]Wu Jiang, Ph.D. thesis, University of Maryland, 1993.

[26]S. N. Mao, X. X. Xi, S. Bhattacharya, Q. Li, T. Venkatesan, J. L. Peng, R. L. Greene, J. Mao, D. H. Wu, S. M. Anlage, Appl. Phys. Lett. **61**, 2356 (1992).

[27]S. N. Mao, X. X. Xi, S. Bhattacharya, Q. Li, J. L. Peng, J. Mao, D. H. Wu, S. M. Anlage, R. L. Greene, and T. Venkatesan, IEEE Trans. Appl. Supercond. **3**, 1552 (1993).

[28]S. N. Mao, X. X. Xi, Jian Mao, D. H. Wu, Q. Li, S. M. An-

[29]S. N. Mao, X. X. Xi, Q. Li, T. Venkatesan, D. Beesabathina, L. Salamanca-Riba, X. D. Wu, J. Appl. Phys. **75**, 2119 (1994).

[30]D. P. Beesabathina, L. Salamanca-Riba, S. N. Mao, X. X. Xi, and T. Venkatesan, Appl. Phys. Lett. **62**, 3022 (1993).

[31]D. P. Beesabathina, L. Salamanca-Riba, S. N. Mao, X. X. Xi, T. Venkatesan, and X. D. Wu (unpublished).

[32]R. Liang, P. Dosanjh, D. A. Bonn, D. J. Barr, J. F. Carolan, and W. N. Hardy, Physica C **195**, 51 (1992).

[33]We thank Dr. Wu Jiang for assistance with this measurement.

[34]T. A. Fiedmann *et al.*, Phys. Rev. B **42**, 6217 (1990).

[35]For single-crystal samples (with the assumption that $X_n = R_n \gg X_s, R_s$), there is a relation between the total change in the bandwidth (δf) and the frequency shift (Δf) of the cavity between the normal and superconducting state: $2\Delta f = \Delta \delta f$. This requirement can be reduced to $X_n(T > T_c) - X_n(T = 0) = R_n(T > T_c) - R_s(T = 0)$ for bulk samples. Our data from single crystals satisfy this condition well. For a detailed discussion see A. M. Portis *et al.*, J. Supercond. **3**, 297 (1990).

[36]W. L. Kennedy, Ph.D. thesis, Northeastern University, 1990.

[37]S. Sridhar and W. Kennedy, Rev. Sci. Instrum. **59**, 531 (1988).

[38]Very near T_c, both measured $\lambda_{\text{meas}}(T)$ and $R_{s,\text{meas}}(T)$ are related to their true bulk values by $\lambda_{\text{meas}} = \lambda_{\text{true}} \tanh(t/2\lambda_{\text{true}})$ and $R_{s,\text{meas}} = R_{s,\text{true}} \tanh(t/2\lambda_{\text{true}})$ due to the size effect from finite film thickness t.

[39]J. P. Turneaure and I. Weissman, J. Appl. Phys. **39**, 4417 (1968).

[40]J. Auer and H. Ullmaier, Phys. Rev. B **7**, 136 (1973).

[41]J. Halbritter, Z. Phys. **266**, 209 (1974).

[42]J. P. Turneaure, J. Halbritter, and H. A. Schwettman, J. Supercond. **4**, 341 (1991).

[43]A. L. Schawlow and G. E. Devlin, Phys. Rev. **113**, 120 (1959).

[44]P. C. L. Tai, M. R. Beasley, and M. Tinkham, Phys. Rev. B **11**, 411 (1975).

[45]W. Schwarz and J. Halbritter, J. Appl. Phys. **48**, 4618 (1977).

[46]Q. Huang, J. F. Zasadzinski, N. Talshawala, K. E. Gray, D. G. Hinks, J. L. Peng, and R. L. Greene, Nature (London) **347**, 369 (1990).

[47]A. Andreone, A. Cassinese, A. DiChiara, R. Vaglio, A. Gupta, and E. Sarnelli, Phys. Rev. B **49**, 6392 (1994).

[48]D. Oates *et al.*, J. Supercond. **3**, 251 (1990).

[49]J. Mao, D. H. Wu, J. L. Peng, R. L. Greene, and S. M. Anlage (unpublished).

[50]S. Skanthakumar, J. W. Lynn, J. L. Peng, and Z. Y. Li, J. Magn. Mag. Mater. **104-107**, 519 (1992).

[51]G. M. Luke *et al.*, Phys. Rev. B **42**, 7981 (1990).

[52]J. W. Lynn, I. W. Sumarlin, D. A. Neumann, J. J. Rush, J. L. Peng, and Z. Y. Li, Phys. Rev. Lett. **66**, 919 (1991).

[53]T. Williams, Y. Maeno, I. Mangelschots, A. Reller, and G. Bednorz, Physica C **161**, 331 (1989).

[54]C. C. Tsuei, Physica A **168**, 238 (1990).

[55]Andreas Kussmaul, Ph.D. thesis, MIT, 1992.

[56]S. J. Hagen, X. Q. Wu, W. Jiang, J. L. Peng, Z. Y. Li, and R. L. Greene, Phys. Rev. B **45**, 515 (1992).

[57]W. Jiang, J. L. Peng, Z. Y. Li, and R. L. Greene, Phys. Rev. B **47**, 8151 (1993).

[58]Beom-hoan O and J. T. Markert, Phys. Rev. B **47**, 8373 (1993).

[59]D. S. Rokhsar, Phys. Rev. Lett. **70**, 493 (1993).

[60]N. Klein, U. Poppe, N. Tellmann, H. Schulz, W. Evers, U. Dahne, and K. Urban, IEEE Trans. Appl. Supercond. **3**, 1102 (1993).

[61]N. Tralshawala, J. F. Zasadzinski, L. Coffey, and Q. Huang, Phys. Rev. B **44**, 12 102 (1991).

[62]H. Chen and J. Callaway, Phys. Rev. B **46**, 14321 (1992).

[63]D. M. King *et al.*, Phys. Rev. Lett. **70**, 3159 (1993).

[64]D. M. Newns, H. R. Krishnamurthy, P. C. Pattnaik, C. C. Tsuei, C. C. Chi, and C. L. Kane, Physica B **186-188**, 801 (1993).

[65]J. M. Getino, M. de Llamo, and H. Rubio, Phys. Rev. B **48**, 597 (1993).

[66]Y. Hidaka and M. Suzuki, Nature (London) **338**, 635 (1989).

[67]X. Q. Xu, S. J. Hagen, W. Jiang, J. L. Peng, Z. Y. Li, and R. L. Greene, Phys. Rev. B **45**, 7356 (1992).

[68]H. D. Drew and K. Stewart (unpublished).